A Promising Thermoelectric Material: Zn_4Sb_3 or $Zn_{6-\delta}Sb_5$. Its Composition, Structure, Stability, and Polymorphs. Structure and Stability of $Zn_{1-\delta}Sb$

Yurij Mozharivskyj,[†] Alexandra O. Pecharsky,[†] Sergey Bud'ko,[†] and Gordon J. Miller*[,‡]

Ames Laboratory, Iowa State University, Ames, Iowa 50011-3020, and Department of Chemistry, Iowa State University, Ames, Iowa 50011-3110

Received December 4, 2003. Revised Manuscript Received February 13, 2004

Composition, crystal structure, and stability of the thermoelectric material, known in the literature as "Zn_4Sb_3", has been characterized using low- and room-temperature single-crystal X-ray diffraction techniques, as well as in situ room- and high-temperature powder X-ray diffraction methods. We have found that the Zn_4Sb_3 phase does not exist below 767 K (the $\beta-\gamma$ transition temperature); it is the $Zn_{6-\delta}Sb_5$ phase that is erroneously assigned the Zn_4Sb_3 composition and is considered to be a promising thermoelectric material. The structure of $Zn_{6-\delta}Sb_5$ is similar to that of "Zn_4Sb_3" but no Zn/Sb mixture is observed on any Sb site. Instead, a significant deficiency on the Zn site is discovered. There are two, not one, as previously reported, $Zn_{6-\delta}Sb_5$ polymorphs below room temperature. In dynamic vacuum and at elevated temperatures the $Zn_{6-\delta}Sb_5$ phase becomes zinc poorer due to zinc sublimation and eventually decomposes into ZnSb and Zn before reaching its melting temperature of 841 K. The binary $Zn_{1-\delta}Sb$ compound also loses zinc in dynamic vacuum and at high temperatures and decomposes into Sb and Zn. The structure of $Zn_{1-\delta}Sb$ (CdSb-type) is analyzed using powder X-ray diffraction techniques.

Introduction

Detailed studies on the Zn_4Sb_3 compound and its cadmium substitutes can be traced back to the 1960s and 1970s and they were fueled by the search for new semiconductors.[1−8] Zn_4Sb_3 was found to have two solid−solid phase transitions: $\alpha \rightarrow \beta$ over the 253−263 K temperature range and $\beta \rightarrow \gamma$ at ∼763 K and to melt congruently at 857 K.[1,2,8] The room-temperature structure of β-Zn_4Sb_3 was originally solved by Bokii et al.[9] (Zn_6Sb_5 X-ray formula) and then by Mayer et al.,[10] who assumed and refined a Zn/Sb mixture on one of the Sb sites to retain the Zn_4Sb_3 composition. The Zn_4Sb_3 formula was universally accepted as a true one despite a very questionable Zn/Sb mixture and earlier reports of the possible existence of Zn_6Sb_5.[8,9] Further research was done by Tapiero et al.[11] in the light of a possible use of Zn_4Sb_3 for photovoltaic solar energy conversion. Using Auger electron spectroscopy, Tapiero et al. found that Zn_4Sb_3 is zinc-deficient ($Zn_{4-\delta}Sb_3$), and has regions of ZnSb and elemental zinc in the microfissures. They also noticed, but did not explain, that annealing of Zn_4Sb_3 in a vacuum at 673 K results in strong impoverishment of Zn (∼27 at. % Zn and ∼83 at. % Sb).

A new wave of research on Zn_4Sb_3 was brought by the discovery of high thermoelectric figures of merit (ZT) in Zn_4Sb_3 between 450 and 670 K ($ZT = 1.3$ at 670 K), which is mostly due to its low thermal conductivity.[12,13] Caillat et al.[12] reported that the compound is stable only up to ∼513 K in the dynamic vacuum. The structure and composition of Zn_4Sb_3 is assumed to be the same as given by Mayer et al.,[10] and neither structural nor another form of quantitative analysis was performed despite the fact that a precise composition is required for future industrial applications. Souma et al.[14] studied thermoelectric performance and other physical properties of Zn_4Sb_3 at low temperatures and found that the

* To whom correspondence should be addressed. E-mail: gmiller@iastate.edu

[†] Ames Laboratory.

[‡] Department of Chemistry.

(1) Ugai, Y. A.; Marshakova, T. A.; Shevchenko, V. Y.; Demina, N. P. *Izv. Akad. Nauk SSSR, Neorg. Mater.* **1969**, *5*, 1381−1385.

(2) Shevchenko, V. Y.; Skripkin, V. A.; Ugai, Y. A.; Marshakova, T. A. *Izv. Akad. Nauk SSSR, Neorg. Mater.* **1968**, *4*, 1359−1360.

(3) Ugai, Y. A.; Marshakova, T. A.; Ignat'ev, N. A.; Aleinikova, K. B. *Tr. Voronezh. Univ.* **1971**, No. 74, 7−10.

(4) Shevchenko, V. Y.; Goncharenko, G. I.; Dvoryankin, V. F.; Ugai, Y. A.; Marshakova, T. A. *Izv. Akad. Nauk SSSR, Neorg. Mater.* **1971**, *7*, 312−313.

(5) Psarev, V. I.; Kirii, V. G. *Izv. Akad. Nauk SSSR, Neorg. Mater.* **1978**, *14*, 1231−1235.

(6) Psarev, V. I.; Kostur, M. L.; Kostur, T. A. *Fiz. Elektron. Respub. Mizhvidom. Nauk.-Tekh. Zb.* **1971**, No. 4, 38−42.

(7) Psarev, V. I.; Kostur, N. L. *Izv. Vyssh. Uchebn. Zaved., Fiz.* **1967**, *10*, 34−38.

(8) Vuillard, G.; Piton, J. P. *C. R. Seances Acad. Sci., Ser. C: Sci. Chim.* **1966**, *263*, 1018−1021.

(9) Bokii, G. B.; Klevtsova, R. F. *Zh. Strukt. Khim.* **1965**, *6*, 866−871.

(10) Mayer, H. W.; Mikhail, I.; Schubert, K. *J. Less-Common Met.* **1978**, *59*, 43−52.

(11) Tapiero, M.; Tarabichi, S.; Gies, J. G.; Noguet, C.; Zielinger, J. P.; Joucla, M.; Loison, J. L.; Robino, M.; Herion, J. *Sol. Energy Mater.* **1985**, *12*, 257−274.

(12) Caillat, T.; Fleurial, J. P.; Borshchevsky, A. *J. Phys. Chem. Solids* **1997**, *58*, 1119−1125.

(13) Caillat, T.; Fleurial, J.-P.; Borshchevsky, A. *Proc. Int. Conf. Thermoelectrics* **1996**, *15th*, 151−154.

(14) Souma, T.; Nakamoto, G.; Kurisu, M. *J. Alloys Compd.* **2002**, *340*, 275−280.

10.1021/cm035274a CCC: $27.50
Published on Web 03/24/2004

α polymorph can be a good thermoelectric material for cryogenic use. They also established the $\alpha \rightarrow \beta$ transition temperature: 257.4 and 236.5 K for samples prepared by gradient-freeze (Bridgman) and sintering methods, respectively. A detailed look at the electrical resistivity plot of one of their samples indicates another phase transition at ~230 K, but it was neither pointed at nor discussed.[14] Further extensive investigation of the Zn−Sb systems and attempts to obtain single-phase Zn_4Sb_3 were done by Izard et al.[15,16] They established the temperature of the $\beta \rightarrow \gamma$ transformation at 767 K and the melting temperature of the γ phase at 841 K and found that the Zn_4Sb_3 phase prepared through mechanical alloying (ball milling) contains Zn, Sb, and ZnSb impurities.

Most of the above-mentioned studies relied on the structural data reported by Mayer et al.,[10] who assumed that the composition of the single crystal must be the same as that of the initial Zn_4Sb_3 sample and, thus, introduced the Zn/Sb mixture on one of the two antimony sites. Two main ways to prepare Zn_4Sb_3 from the melt are quenching a liquid mixture to room temperature[1,10−12] or slowly cooling the melt below the $\gamma \rightarrow \beta$ transition temperature and, subsequently, quenching or slowly cooling the alloy to room temperature.[11,14] As indicated by Tapiero et al.,[11] the two approaches lead to unique crystallized phase Zn_4Sb_3. In this paper we reported on the crystal structure, composition, stability, and polymorphs of the "Zn_4Sb_3" phase prepared by the latter technique.

Experimental Section

Synthesis. The starting materials were pieces of zinc (99.99 wt %, Alfa Aesar) and antimony (99.999 wt %, Alfa Aesar). The stoichiometric Zn_4Sb_3 mixture of the elements with a total mass of 2 g was sealed in an evacuated silica tube and heated to 973 K in 2 h. A liquid solution, obtained at that temperature, was periodically shaken to ensure proper mixing of the constituents during the annealing time of 4 h. The mixture was then cooled in 1 h from 973 to 758 K, below the $\gamma \rightarrow \beta$ transition temperature of 767 K,[15] annealed at 758 K for 1 h, and then quenched in cold water. The annealing temperatures were stable within ±2 K with respect to the values set for an experiment. The alloy was metallic and shiny in appearance and contained small crystals.

An alloy with the $Zn_{3.6}Sb_3$ or Zn_6Sb_5 composition was prepared the same way (a full occupancy of the Zn site and no Zn/Sb mixture are assumed).

Resistance Measurements. The resistance measurement on the Zn_4Sb_3 sample was performed in the 4−350 K range to establish the $\alpha \rightarrow \beta$ transition temperature and possibly the nature of the transition. A standard four-probe method (an ACT option of a PPMS9 instrument) was used; contacts to the sample were made with Epotek H20E silver epoxy and Pt wires. The heating and cooling were done at the rate of less than 0.5 K/min, and the resistance value was recorded every 2 degrees. To explore the nature of the transformation, the sample was cycled three times through the transition temperature.

As apparent from Figure 1, there exist two separate transitions: one at 252−256 K (differentiation gives T_t = 254 K) and another at 232−234 K. The first transition is likely to be a second-order one since it exhibits no hysteresis during cycling and its steep drop in resistance resembles the right side of a

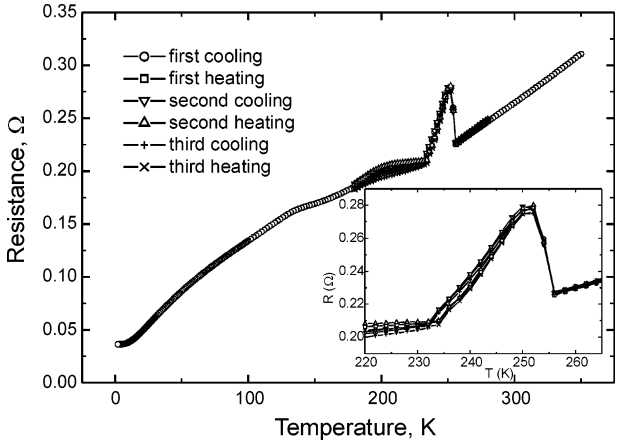

Figure 1. Resistance of the Zn_4Sb_3 alloy as a function of temperature. The insert shows the transition region.

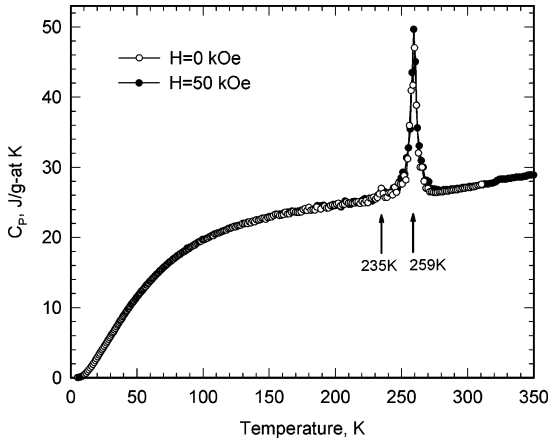

Figure 2. Heat capacity of the Zn_4Sb_3 sample measured from ~5 to 310 K in the 0 kOe magnetic field and from 80 to 350 K in the 50 kOe magnetic field. The arrows indicate the phase transitions at 235 and 259 K.

λ-type second-order transition. The newly formed phase is stable in a rather narrow temperature interval between 256 and 232 K, below which it transforms into another polymorph. The second transition bears two features of a first-order phase transition: the presence of hysteresis upon heating (T_t = 234 K) and cooling (T_t = 232 K) and a sudden change in the slope of resistance versus temperature. A generalized look at the two transformations creates an impression of only one λ-type second-order transition, but detailed analysis, outlined above, heat capacity, and crystallographic data, given below, clearly indicate two separate transitions.

Heat Capacity Measurements. To verify the presence of a low-temperature phase transition, heat capacity (c_p) measurements were performed on the Zn_4Sb_3 alloy using a semiadiabatic heat pulse calorimeter in constant magnetic fields of 0 and 50 kOe between ~5 and 350 K with a heating rate of 0.5 K/min.[17] As apparent from Figure 2, there are indeed two separate phase transitions: one at 259 K and another at 235 K. The large peak in c_p at 259 K indicates a transition, which is known in the literature as the $\alpha \rightarrow \beta$ transition. The small peak in c_p at 235 K proves the existence of another transition that was discovered during our resistance measurements. While the transition temperature (T_t) of the low-temperature transformation can be different on cooling (there is hysteresis in resistance upon cooling and heating), the T_t temperature of the high-temperature transformation is most likely to remain the same (no hysteresis in resistance upon cycling). Application of the magnetic field (H = 50 kOe) did not affect

(15) Izard, V.; Record, M. C.; Tedenac, J. C. *J. Alloys Compd.* **2002**, *345*, 257−264.

(16) Izard, V.; Record, M. C.; Tedenac, J. C.; Fries, S. G. *CALPHAD: Comput. Coupling Phase Diagrams Thermochem.* **2002**, *25*, 567−581.

(17) Pecharsky, V. K.; Moorman, J. O.; Gschneider, K. A., Jr. *Rev. Sci. Instrum.* **1997**, *68*, 4196−4207.

Table 1. Crystal Data and Structure Refinements of the $Zn_{6-\delta}Sb_5$ Single Crystal from the Zn_4Sb_3 Sample

temperature, K	293(1)	203(1)[a]
composition	$Zn_{5.38(2)}Sb_5$ ($Zn_{3.23(1)}Sb_3$)	$Zn_{5.24(5)}Sb_5$ ($Zn_{3.15(3)}Sb_3$)
space group (Pearson symbol)	$R\bar{3}c$ (*hR*22)	*R*32 (*hR*22)
lattice parameters, Å	$a = 12.2288(6)$	$a = 12.246(1)$
	$c = 12.422(1)$	$c = 12.433(2)$
volume, Å^3	1608.8(2)	1614.5(3)
Z	6	6
diffractometer	SMART Apex	SMART 1000
wavelength, Å (Mo Kα radiation)	0.71073	0.71073
2θ range	6.66−56.56°	5.04−56.46°
index ranges	$-16 \le h \le 16$, $-16 \le k \le 15$, $-16 \le l \le 16$	$-16 \le h \le 11$, $-9 \le k \le 16$, $-16 \le l \le 16$
independent reflections	438 ($R_{int} = 0.0259$)	840 ($R_{int} = 0.0971$)
completeness to $2\theta_{max}$	96.3%	94.9%
data/parameters	438/20	840/37
goodness-of-fit on F^2	1.094	1.274
final *R* indices [$I/\sigma(I) > 2$]	R1 = 0.0296, wR2 = 0.0751	R1 = 0.0743, wR2 = 0.1540
R indices (all data)	R1 = 0.0307, wR2 = 0.0758	R1 = 0.0832, wR2 = 0.1585
extinction coefficient	0.00027(5)	0.00022(5)
largest diff. peak/hole, e/Å^3	2.296/−0.998	3.617/−3.453

[a] Crystallographic data at 203 K are for the basic structure.

the transition temperatures, which indicates that the two transformations are not accompanied by a magnetic ordering. This is an expected result since a fully filled d-shell of Zn atoms (d^{10} configuration) precludes magnetic ordering.

The T_t temperatures of 235 and 259 K are obtained during heating the alloy and are 1 and 5 K higher than the corresponding T_t temperatures of 234 and 254 K obtained from the resistance measurements upon heating. Differences in the T_t temperatures, obtained from the two methods, are likely to result from different sizes of the samples and different techniques used.

X-ray Analyses. *Room-Temperature Single Crystal and Powder X-ray Diffraction Studies.* The Zn_4Sb_3 sample was characterized by room-, low-, and high-temperature single crystal and powder X-ray diffraction (XRD) techniques. Crystals were extracted from the stoichiometric Zn_4Sb_3 sample and checked for crystal quality by the Laue method (Cu Kα radiation). After the initial screening three crystals with dimensions 30−40 × 45−55 × 60−65 μm^3 were selected for further analysis. Room-temperature single-crystal diffraction data were collected on a Bruker Apex CCD diffractometer in a full reciprocal sphere with 0.3° scans in ω and with an exposure time of 10−15 s/frame. Intensities were extracted and then corrected for Lorentz and polarization effects through the SAINT program.[18] Empirical absorption corrections were based on modeling a transmission surface by spherical harmonics employing equivalent reflections with $I > 3\sigma(I)$ (program SADABS).[18]

Analysis of the reflections indicated an observed rhombohedral unit cell and presence of a *c* glide plane ($R\bar{3}c$ space group). Structures of the crystals from the Zn_4Sb_3 sample were solved by direct methods and refined on F^2 by the full-matrix least-squares method in its own "Zn_4Sb_3" type (crystallographic data for one of the crystals are presented in Tables 1, 2, and 3). Contrary to the previous structural data,[10] no Zn/Sb statistical mixture was found on the 18e site in any of the three studied crystals. However, large temperature factors were observed for the Zn atoms, site 36f, in all crystals, which is indicative of partial site occupancy. Relaxing the occupancy parameter resulted in reasonable U_{eq} values and lower R_1 factors (e.g., 0.0296 instead of 0.0344 for one of the crystals). The Hamilton test[19] indicates that a full Zn occupancy can be rejected at a lower than 0.005 probability level. Occupancies of the two Sb sites were also tested, but no statistically significant deviations from unity were detected (e.g., 0.994(7) for Sb1 and 1.005(8) for Sb2 in one of the crystals). The refined compositions for the three crystals are as follows: (1) $Zn_{3.23(1)}Sb_3$ or $Zn_{5.38(2)}Sb_5$ ($R_1 = 0.0296$), (2) $Zn_{3.22(1)}Sb_3$ or $Zn_{5.37(2)}Sb_5$ ($R_1 = 0.0323$), and (3) $Zn_{3.21(2)}Sb_3$ or $Zn_{5.35(4)}Sb_5$ ($R_1 = 0.0341$); and are within 1 standard deviation from one another.

Table 2. Atomic and Equivalent Isotropic Displacement Parameters[a] (U_{eq}, Å^2) for the $Zn_{6-\delta}Sb_5$ Single Crystal from the Zn_4Sb_3 Sample

atom		occup.	*x*/*a*	*y*/*b*	*z*/*c*	U_{eq}
			293 K			
Zn	36f	0.896(4)	0.24416(9)	0.07927(9)	0.09655(8)	0.0255(3)
Sb1	18e	1	0.35590(5)	0	1/4	0.0163(2)
Sb2	12c	1	0	0	0.13644(5)	0.0158(2)
			203 K			
Zn1	18f	0.874(9)	0.0707(4)	0.2407(4)	0.1501(3)	0.017(1)
Zn2	18f	0.874(9)	0.2490(4)	0.1629(4)	0.3427(3)	0.0153(9)
Sb1	9e	1	0.6442(2)	0	1/2	0.0105(6)
Sb2	9d	1	0.3576(3)	0	0	0.0155(7)
Sb3	6c	1	0	0	0.1123(2)	0.0100(7)
Sb4	6c	1	0	0	0.3845(3)	0.0178(8)

[a] Anisotropic temperature factors and other crystallographic details can be obtained from the authors upon request.

Table 3. Selected Interatomic Distances in Room-Temperature $Zn_{6-\delta}Sb_5$ (Single-Crystal Data)

atoms	distance, Å	atoms	distance, Å
Zn−Zn	2.777(2)	Sb1−2Zn	2.727(1)
Sb2	2.6866(9)	Sb1−2Zn	2.789(1)
Sb1	2.727(1)	Sb1−2Zn	2.797(1)
Sb1	2.789(1)		
Sb1	2.797(1)	Sb2−3Zn	2.6866(9)
		Sb2	2.824(1)

Deviation from the stoichiometric composition was tested on the bulk Zn_4Sb_3 alloy using powder XRD (Huber image plate camera, Tables 4 and 5). Within sensitivity limits of the powder XRD method the Zn_4Sb_3 sample contained the "Zn_4Sb_3"-type phase (98.3(2) wt %), elemental zinc (1.72(4) wt %) as an impurity and a small amount of another, presumably metastable Zn_3Sb_2 phase (Figure 3a). Due to the lack of structural data on Zn_3Sb_2, we could not prove its presence in the sample and, therefore, refine its amount (Psarev et al. reported only on quenching Zn_3Sb_2, stable above ~687 K, to room temperature[20]). The refinement yielded a nonstoichiometric composition $Zn_{3.384(7)}Sb_3$, which is richer in zinc than the compositions from the single-crystal data, but is still far from the stoichiometric Zn/Sb ratio of 4:3.

X-ray powder diffraction on the $Zn_{3.6}Sb_3$ (Zn_6Sb_5) sample, prepared the same way as the Zn_4Sb_3 alloy and on the assumption of full occupancy of the Zn site, indicated the presence of the "Zn_4Sb_3"-type phase with a refined composition

(18) *XRD Single Crystal Software*; Bruker Analytical X-ray Systems: Madison, WI, 2002.

(19) Hamilton, W. C. *Acta Crystallogr.* **1965**, *18*, 502−510.

(20) Psarev, V. I.; Kirii, V. G.; Andronnikov, V. A. *Izv. Akad. Nauk SSSR, Neorg. Mater.* **1981**, *17*, 396−401.

Table 4. Powder Refinement Data of the Dominant Phases at the Selected Temperatures during Heating of the Zn_4Sb_3 Sample

temperature	293(1) K	673(2) K	793(2) K
composition	$Zn_{5.64(1)}Sb_5$ ($Zn_{3.384(7)}Sb_3$)	$Zn_{0.960(4)}Sb$	Sb
space group (Pearson symbol)	$R\bar{3}c$ ($hR22$)	$Pbca$ ($oP16$)	$R\bar{3}m$ ($hR2$)
lattice parameters, Å	$a = 12.23458(4)$ $c = 12.43005(7)$	$a = 6.2501(3)$ $b = 7.7758(3)$ $c = 8.1188(4)$	$a = 4.33185(8)$ $c = 11.3742(4)$
volume, Å^3	1611.32(1)	394.57(3)	184.814(8)
Z	6	8	6
X-ray machine	Huber image plate	Rigaku diffractometer	Rigaku diffractometer
wavelength	Cu Kα_1	Mo Kα_1 and Mo Kα_2	Mo Kα_1 and Mo Kα_2
2θ and step	20°−80°, 0.005°	8°−45°, 0.01°	8°−45°, 0.01°
reflections	115	513	86
fitted parameters	26	21	16
refinement, program	Rietveld, Rietica	Rietveld, Rietica	Rietveld, Rietica
$R_I = \Sigma\|I_o - I_c\|/\Sigma\|I_o\|$	0.025	0.052	0.039
$R_P = \Sigma\|y_{oi} - y_{ci}\|/\Sigma\|y_{oi}\|$	0.038	0.104	0.113
$R_{wP} = (\Sigma w_i(y_{oi} - y_{ci})^2/ \Sigma w_i(y_{oi})^2)^{1/2}$ [a]	0.049	0.140	0.149

[a] $w_i = (y_{oi})^{-1/2}$.

Table 5. Atomic and Isotropic Thermal (B_{iso}, Å^2) Parameters for the Dominant Phases upon Heating the Zn_4Sb_3 Sample (Powder Diffraction Data)

atom		occup.	x/a	y/b	z/c	B_{iso}
			$Zn_{6-\delta}Sb_5$, 293 K			
Zn	36f	0.940(2)	0.24438(9)	0.08041(8)	0.09594(8)	1.11(3)
Sb1	18e	1	0.35672(5)	0	$^1/_4$	0.25(2)
Sb2	12c	1	0	0	0.13721(6)	0.44(2)
			$Zn_{1-\delta}Sb$, 673 K			
Zn	8c	0.960(4)	0.4562(4)	0.1137(3)	0.8676(4)	1.35(7)
Sb	8c	1	0.1431(2)	0.0821(2)	0.1095(2)	0.49(3)
			Sb, 893 K			
Sb	6c		0	0	0.26629(7)	1.79(2)

of $Zn_{3.316(7)}Sb_3$ (66.2(1) wt %) and a secondary binary phase ZnSb (33.8(1) wt %) (Figure 3b). From the Rietveld refinement, the ZnSb phase (*Pbca*, $a = 6.20393(8)$ Å, $b = 7.7408(1)$ Å, and $c = 8.0977(1)$ Å) crystallizes with the CdSb-type structure,[21] and it appears to have fully occupied Zn and Sb sites at room temperature (Zn: $x = 0.4580(3)$ Å, $y = 0.1104(3)$ Å, $z = 0.8673(4)$ Å, $B = 1.5(1)$ Å^2, $n = 1.013(5)$; Sb: $x = 0.1416(2)$ Å, $y = 0.0822(2)$ Å, $z = 0.1090(2)$ Å, $B = 1.28(5)$ Å^2, $n = 1.002(4)$).

As evident from the single crystal and powder XRD data, the Zn concentration in the "Zn_4Sb_3"-type phase is much less than the amount presented by the stoichiometric Zn_4Sb_3 formula. Even if the Zn position were fully occupied, its formula should be written as $Zn_{3.6}Sb_3$ or Zn_6Sb_5, but not as Zn_4Sb_3. It is well-known that powder and, especially, single-crystal X-ray diffraction methods are among the most reliable analytical tools to determine a composition of a bulk crystalline material when atomic numbers of the constituents are quite different (this is the case for the Zn_4Sb_3 sample). Thus, we conclude that the Zn_4Sb_3 phase as such does not exist, but it is the deficient $Zn_{6-\delta}Sb_5$ phase that forms in the Zn_4Sb_3 sample and is mistakenly assigned the Zn_4Sb_3 composition. We will use the general Zn_4Sb_3 formula, when we refer to the initial composition of the sample, but we will use the $Zn_{6-\delta}Sb_5$ formula when we refer to the phase itself or its polymorphs or emphasize a refined composition or Zn occupancy.

Low-Temperature Single-Crystal XRD Studies. The low-temperature (203, 223, and 243 K) data for the first crystal were taken on a Bruker SMART 1000 CCD diffractometer with Mo Kα radiation. During the low-temperature experiments the temperature was stable within ±1 K with respect to the value set for an experiment. Diffraction data were collected and processed the same way as the room-temperature ones. Indexing and analysis of the reflections at 243 K for the $Zn_{6-\delta}Sb_5$ polymorph stable between 232 and 256 K yielded a rhombohedral unit cell with $a = 12.2250(8)$ Å and $c = 12.4257(15)$ Å (hexagonal setting) and the $R\bar{3}c$ space group. No additional Bragg reflections that could indicate the presence of a superstructure or change in symmetry were observed. Structure solution and refinement gave a $Zn_{5.38(6)}Sb_5$ formula and atomic positions analogous to the room-temperature ones (they are within 3 standard deviations from one another and are not presented here). Shapes of thermal ellipsoids at 243 K were analogous to those at room temperature. Thus, present structural data do not provide an answer to changes in the resistance at 254 K and heat capacity at 259 K.

Lowering the temperature further to 203 K yielded a low-temperature polymorph of $Zn_{6-\delta}Sb_5$: monoclinic *C*-centered cell with $a_m = 32.570(4)$, $b_m = 12.246(1)$, $c_m = 10.855(1)$ Å, $\beta_m = 99.100(2)°$, and 16 formula units. If only the main reflections were considered, a basic, average rhombohedral unit cell with $a_h = 12.246(1)$ Åand $c_h = 12.433(2)$ Å (hexagonal setting) was obtained. The axial transformation between the two cells can be presented in matrix form:

$$\begin{pmatrix} \vec{a}_m \\ \vec{b}_m \\ \vec{c}_m \end{pmatrix} = \begin{pmatrix} -2 & -1 & -2 \\ 0 & -1 & 0 \\ -^2/_3 & -^1/_3 & ^2/_3 \end{pmatrix} \begin{pmatrix} \vec{a}_h \\ \vec{b}_h \\ \vec{c}_h \end{pmatrix}$$

Violation of the extinction condition $l = 6n$ for the $00l$ reflections for the smaller cell undoubtedly indicated loss of the *c* glide plane. The basic structure was solved by direct methods and refined in the *R*32 space group (Tables 1 and 2; other rhombohedral space groups were also tested, but they did not give satisfactory results). During the refinement, the occupancy factors of the two Zn sites were set equal because of the correlation effect, which affected occupancies, and also due to the fact that redistribution of Zn atoms is unlikely to occur at such low temperatures. The refined $Zn_{5.24(5)}Sb_5$ composition of this low-temperature average structure is similar within 3 standard deviations to the compositions obtained at 293 and 243 K. Crystallographic data for this polymorph were also taken at 223 K, which are similar to those at 203 K and are not presented (except for the lattice parameters of the basic cell in Table 6). One of the unusual features of the low-temperature phase is that the dimensions of its basic cell and, correspondingly, its volume are larger than those of the next two polymorphs at 243 and 293 K (Table 6). Application of direct methods to the larger monoclinic cell was unsuccessful. Further attempts to solve and refine the full structure, using a "modulated" approach and a superspace formalism,[22] are currently underway.

High-Temperature Single-Crystal XRD Studies. The high-temperature (473, 673, and 803 K) data for the first $Zn_{6-\delta}Sb_5$ crystal were taken on a Bruker SMART Apex CCD diffractometer with Mo Kα radiation, equipped with a Nonius crystal heater (±1 K temperature stability). To prevent crystal contamination at high temperatures, neither glue nor cement

(21) Almin, K. E. *Acta Chem. Scand.* **1948**, *2*, 400−407.

(22) Van Smaalen, S. *Crystallogr. Rev.* **1995**, *4*, 79−202.

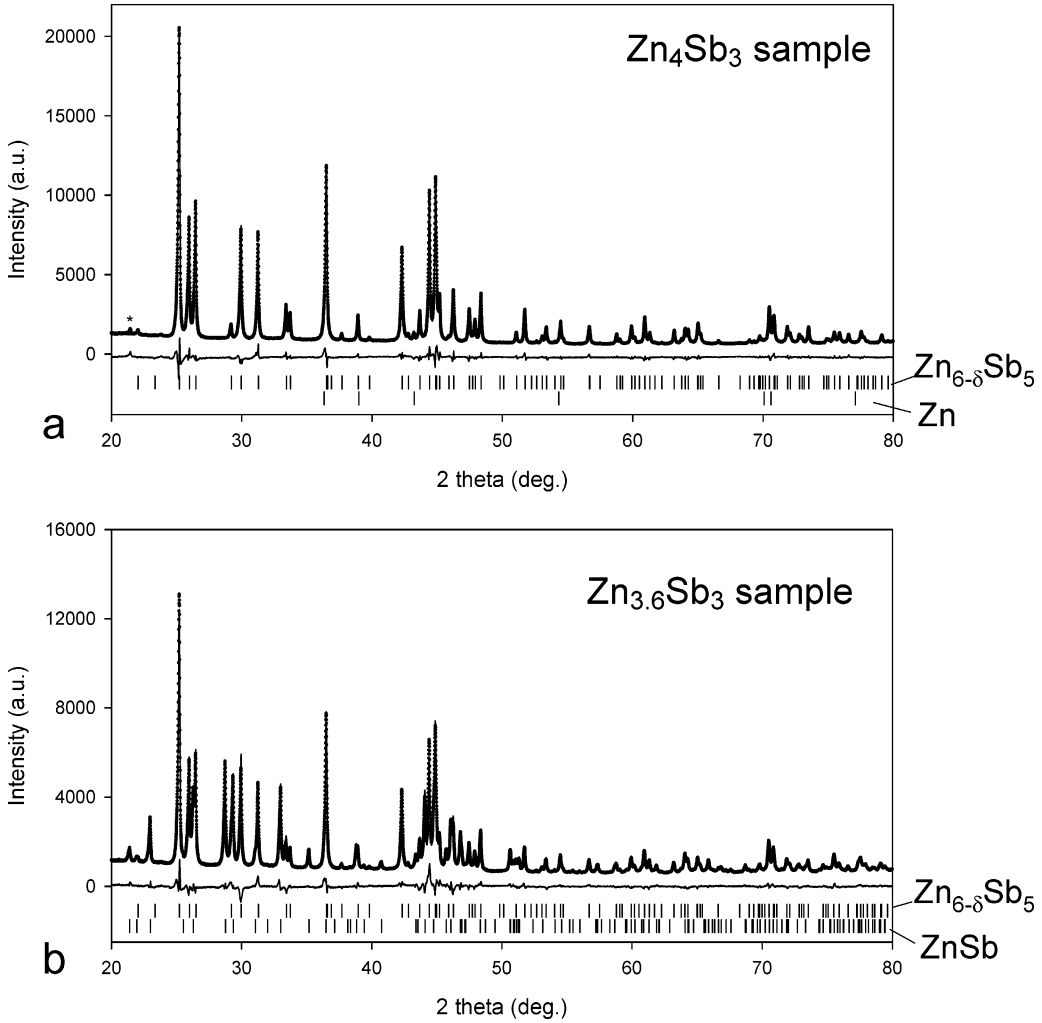

Figure 3. Rietveld refinements of the identified phases in the Zn_4Sb_3 (a) and $Zn_{3.6}Sb_3$ (b) samples. The X-ray diffraction data were collected at room temperature. Dots and two solid lines represent observed and calculated profiles and the difference between them, respectively. The vertical bars show positions of Bragg peaks. An asterisk at $2\theta = \sim 21°$ (a) indicates a reflection of an unidentified phase.

was used to mount the crystal. The crystal was placed at the bottom of a 0.2-mm capillary and fixed in place by a smaller 0.1-mm capillary. Since the mounting was done in air, freshly prepared Gd filings (getter) were put on top of the inner 0.1-mm capillary to bind oxygen during heating (to avoid crystal oxidation). The outer 0.2-mm capillary was sealed using a microtorch and then mounted in a 0.9-mm stainless steel tube using temperature-resistant cement. Three sets of 30 frames with 0.3° scans in ω and with an exposure time of 10 s/frame were collected to obtain lattice parameters at various temperatures.

Indexing and subsequent least-squares refinement of reflections collected at 473 K yielded a rhombohedral unit cell with $a = 12.271(3)$ Å and $c = 12.472(2)$ Å (hexagonal setting). After raising the temperature to 673 K, the $Zn_{6-\delta}Sb_5$ crystal broke into small pieces, Bragg reflections of which were weak and overlapped. Nevertheless, lattice parameters (rhombohedral unit cell) for the largest piece could be obtained: $a = 12.230(4)$ Å and $c = 12.498(2)$ Å (hexagonal setting). While an increase in the c parameter with temperature is expected, a decrease in the a parameter is not understood. Further heating to 803 K, above the $\beta \rightarrow \gamma$ transition temperature of 767 K,[15] resulted in the formation of a new phase, presumably the γ-polymorph. Indexing the reflections from the broken crystal (program Gemini[18]) gave a trigonal/hexagonal unit cell: $a = 14.89(2)$ Å and $c = 7.85(2)$ Å. At that point diffraction data were collected in a reciprocal hemisphere at 803 K, but because of the weak intensities and reflections' overlap, we could not reliably determine a space group, solve, and refine the structure.

High-Temperature Powder XRD Studies. The high-temperature data on the properly ground Zn_4Sb_3 sample were collected on a Rigaku TTRAX rotating anode diffractometer (Mo Kα radiation, $8 \leq 2\theta \leq 45°$, 0.01° step, 1 s/step scanning time, 10^{-7} Torr dynamic vacuum, ± 2 K temperature stability, 293−873 K temperature range). The diffraction profiles are compiled in Figure 4. The $Zn_{6-\delta}Sb_5$ phase ($R\bar{3}c$ space group) is observed up to 693 K; at 623 K a new phase develops, which remains up to 753 K; at 693 K another phase appears that is stable up to 873 K.

It is well-established that the $Zn_{6-\delta}Sb_5$ phase, known as "Zn_4Sb_3", melts congruently at 841 K.[15,16] Presence of the crystalline phase in our sample at 873 K indicated that we are dealing with a different compound. The structure of this "high-temperature" phase was solved using a direct-method approach. At the beginning the powder pattern at 793 K was automatically indexed in the hexagonal unit cell with $a = 4.331$ and $c = 11.373$ Å (program INDP from the CSD package).[23] Analysis of the observed Bragg reflections undoubtedly indicated a rhombohedral unit cell and absence of a c glide plane. The structure was then successfully solved (program MULTAN)[23] and refined (program Rietica,[24] Tables 4 and 5,

(23) Akselrud, L. G.; Grin, Y. M.; Pecharsky, V. K.; Zavalij, P. Y. In *Proceedings 12th European Crystallographic Meeting*; Kristallographiya, Suppl.; Academy of Sciences: Moscow, USSR, 1989; Vol. 155, pp 2−3.

(24) Hunter, B. A.; Howard, C. J. *Rietica*; Australian Nuclear Science and Technology Organization: Menai, Australia, 2000.

Table 6. Crystallographic Data and Refined Compositions (if can be obtained reliably) of the Phases in the Zn_4Sb_3 Sample at Different Temperatures. Amount of Each Phase Is in Weight Percents (accuracy < 1%) and Is Given in Parentheses after the Composition

T, K	space group	method	composition	*a*, Å	*b*, Å	*c*, Å	*V*, Å^3
203	$R32$	s.c.[a]	$Zn_{5.24(5)}Sb_5$ (100)	12.246(1)		12.433(2)	1614.5(3)
223	$R32$	s.c.	$Zn_{5.21(6)}Sb_5$ (100)	12.2397(9)		12.420(2)	1611.4(3)
243	$R\bar{3}c$	s.c.	$Zn_{5.38(6)}Sb_5$ (100)	12.2250(8)		12.426(2)	1608.2(2)
293	$R\bar{3}c$	s.c.	$Zn_{5.38(2)}Sb_5$ (100)	12.2288(6)		12.422(1)	1608.8(2)
	$R\bar{3}c$	powder	$Zn_{5.64(1)}Sb_5$ (98)	12.23458(4)		12.43005(7)	1611.32(1)
	$P6_3/mmc$		Zn (2)	2.6666(2)		4.946(1)	30.459(7)
373	$R\bar{3}c$	powder	$Zn_{5.72(2)}Sb_5$ (100)	12.2581(4)		12.4545(7)	1620.7(1)
473	$R\bar{3}c$	powder	$Zn_{5.61(2)}Sb_5$ (100)	12.2771(4)		12.4721(6)	1628.0(1)
573	$R\bar{3}c$	powder	$Zn_{5.54(2)}Sb_5$ (100)	12.2835(4)		12.4801(8)	1630.8(1)
623	$R\bar{3}c$	powder	$Zn_{5.43(2)}Sb_5$ (74)	12.2983(4)	7.765(1)	12.5002(6)	1637.3(1)
	$Pbca$		ZnSb (26)	6.2433(9)		8.116(1)	393.5(1)
673	$R\bar{3}c$	powder	$Zn_{6-\delta}Sb_5$ (15)	12.311(1)	7.7758(3)	12.508(2)	1641.7(3)
	$Pbca$		$Zn_{0.960(4)}Sb$ (85)	6.2501(3)		8.1188(4)	394.57(3)
693	$R\bar{3}c$	powder	$Zn_{6-\delta}Sb_5$ (3)	12.326(3)	7.7796(3)	12.470(6)	1641(1)
	$Pbca$		$Zn_{0.964(4)}Sb$ (86)	6.2534(3)		8.1207(4)	395.06(3)
	$R\bar{3}m$		Sb (11)	4.3235(4)		11.339(2)	183.56(4)
713	$Pbca$	powder	$Zn_{0.964(4)}Sb$ (69)	6.2566(3)	7.7818(4)	8.1222(4)	395.45(3)
	$R\bar{3}m$		Sb (31)	4.3265(2)		11.3518(9)	184.02(2)
733	$Pbca$	powder	$Zn_{0.955(7)}Sb$ (37)	6.2641(5)	7.7876(6)	8.1284(7)	396.53(6)
	$R\bar{3}m$		Sb (63)	4.3265(2)		11.3518(9)	184.02(2)
753	$Pbca$	powder	$Zn_{1-\delta}Sb$ (8)	6.271(2)	7.793(2)	8.135(2)	396.7(2)
	$R\bar{3}m$		Sb (92)	4.32943(9)		11.3631(4)	184.454(8)
763	$R\bar{3}m$	powder	Sb (100)	4.3302(1)		11.3646(5)	184.55(1)
773	$R\bar{3}m$	powder	Sb (100)	4.32866(9)		11.3615(4)	184.363(8)
793	$R\bar{3}m$	powder	Sb (100)	4.33185(8)		11.3742(4)	184.814(8)
813	$R\bar{3}m$	powder	Sb (100)	4.33223(8)		11.3780(4)	184.835(8)
873	$R\bar{3}m$	powder	Sb (100)	4.3350(2)		11.3900(8)	185.37(2)

[a] s.c. stands for single crystal.

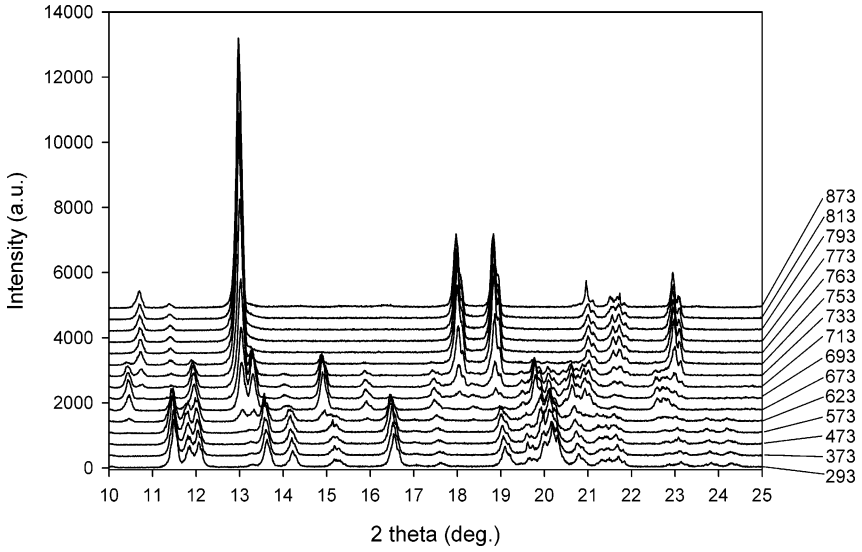

Figure 4. X-ray powder diffraction patterns of the Zn_4Sb_3 sample during heating from 293 to 873 K. Only the $2\theta = 10-25°$ regions are shown.

Figure 5c) in a high-symmetry space group $R\bar{3}m$. The structure is essentially that of room-temperature antimony[25] but it has a slightly different atomic *z* parameter (0.26629 instead of 0.23349). Since the unit cell contains only one atomic position, the Sb/Zn ratio could not be refined. Although small solubility of zinc in antimony cannot be excluded, especially at high temperatures, we assume only Sb atoms in the structure, based on the literature data.[15]

Appearance of antimony as a final product suggests that the intermediate phase during heating might be ZnSb. Indeed, this binary phase was identified and successfully refined at different temperatures. Figure 5a,b presents Rietveld refinements of $Zn_{1-\delta}Sb$ in the presence of $Zn_{6-\delta}Sb_5$ at 673 K and of Sb at 733 K, respectively, and Tables 4 and 5 give crystallographic data and refinement results for $Zn_{1-\delta}Sb$ at 673 K. As indicated before, the structure of $Zn_{1-\delta}Sb$ is similar to that of CdSb.[21] At room temperature and 623 K no deficiency on the Zn site was detected, but at 673−713 K there is a statistically significant deviation from unity.

EDS Analysis. Energy dispersive spectroscopy (EDS) quantitative analysis of five crystals from the Zn_4Sb_3 alloy was performed on a JEOL 840A scanning electron microscope, equipped with an IXRF Systems Iridium X-ray analyzer. The experiment yielded the following Zn/Sb ratios (in at. %): 58.7(7)/41.3(7), 60.6(7)/39.4(7), 60.1(7)/39.9(7), 59.2(7)/40.8(7), and 59.8(7)/40.2(7). The results indicate that the surface (the outer ~500-nm layer) of the crystals is richer in Zn, not just as compared to the XRD composition of the crystals (the stoichiometric Zn_6Sb_5 formula gives the Zn/Sb ratio of 54.5/45.5 at. %) but also as compared to the initial composition of the Zn_4Sb_3 sample (Zn/Sb = 57.1/42.9 at. %). In fact, the

(25) Barrett, C. S.; Cucka, P.; Haefner, K. *Acta Crystallogr.* **1963**, *16*, 451−453.

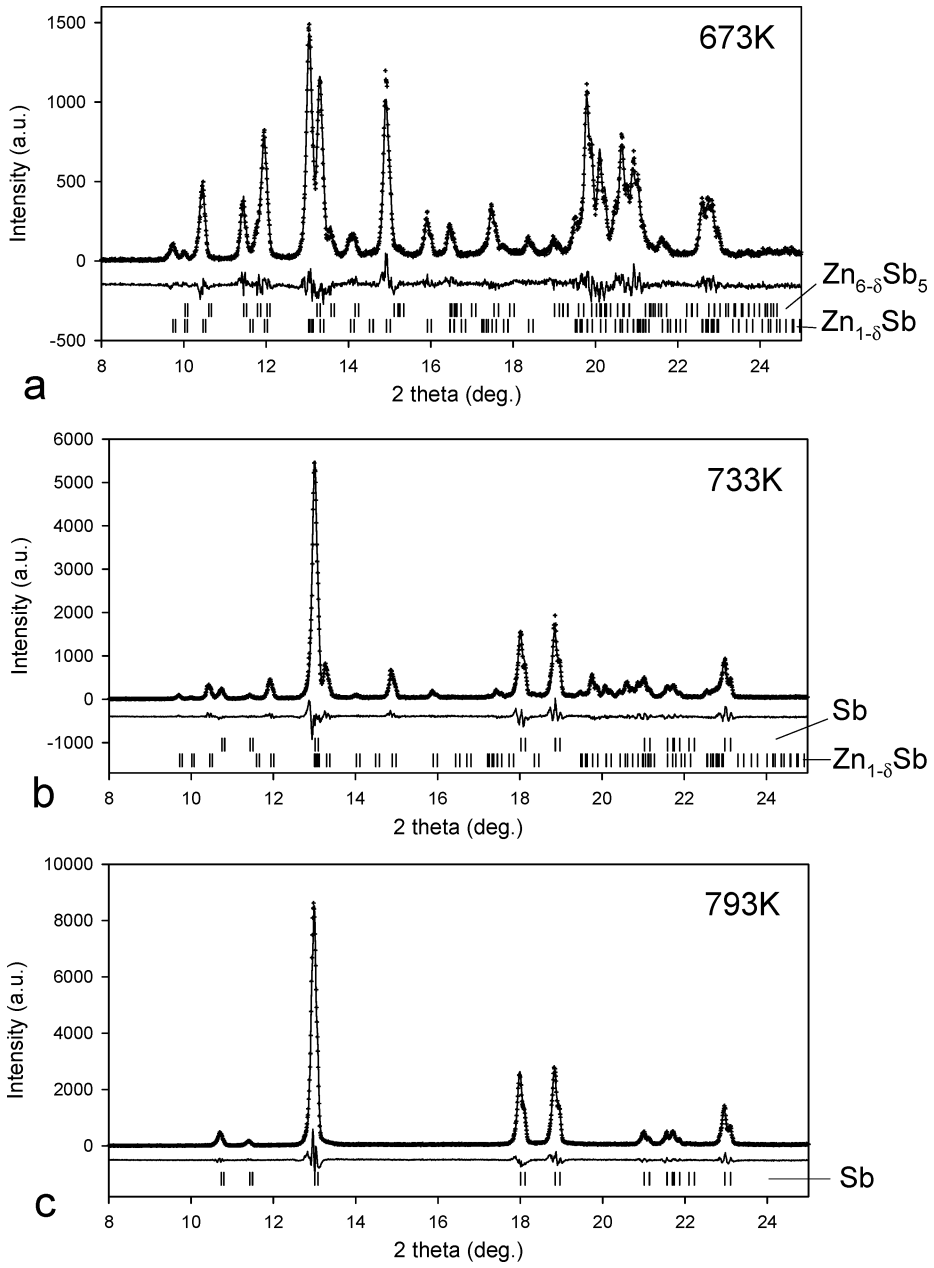

Figure 5. Rietveld refinements of the phases in the Zn_4Sb_3 sample at 673 (a), 733 (b), and 793 K (c). Dots and two solid lines represent observed and calculated profiles and the difference between them, respectively. Vertical bars show positions of Bragg peaks. Only the $2\theta = 8-25°$ regions are shown.

average experimental Zn/Sb ratio of 59.7/40.3 at. % corresponds well to the Zn_3Sb_2 formula. While it can be speculated whether the zinc enrichment of crystal surfaces is due to a Zn_3Sb_2 layer, it is clear that the surface is much zinc-richer than the bulk of a crystal. This unusual phenomenon was also observed by Tapiero et al.,[11] who using Auger electron spectroscopy noticed significant deviation in the Zn/Sb ratio on the surface of a Zn_4Sb_3 alloy: the first 10−20-Å layer has a composition close to Zn_3Sb_2 (as judged from the plot). Although the resolution of the EDS method in terms of the penetration depths (very thin layers cannot be analyzed) is much smaller than that of the Auger electron spectroscopy (composition of an ∼10-Å layer can be evaluated), the two methods undoubtedly indicate a larger amount of Zn on the surface of the Zn_4Sb_3 alloy.

Results and Discussion

Phase Transitions and Stability of $Zn_{6-\delta}Sb_5$ and $Zn_{1-\delta}Sb$. Phase analysis, refined compositions, and crystallographic data of the phases identified in the Zn_4Sb_3 sample at different temperatures are compiled in Table 6. Our structural data and resistance measurements indicate that there are three $Zn_{6-\delta}Sb_5$ polymorphs below room temperature: α below 232 K, another polymorph, called α′ thereafter, between 232 and 256 K, and β from 256 K up. As discussed above, the α → α′ transformation, which was not reported before, is a first-order one. The α′ → β transition is likely to be a second-order one, and its temperature of 256 K is close to that of 257.4 K found in the literature and defined as an α → β transition point.[14] The present single-crystal XRD data indicate no structural changes during the α′ → β transformation, although the resistance and heat capacity measurements undoubtedly indicate a phase transition. Therefore, more work, involving high-resolution powder diffraction, has to be

done to check for a possible symmetry change and to obtain a better understanding of this phenomenon.

If the refined compositions from the bulk Zn_4Sb_3 and $Zn_{3.6}Sb_3$ samples are taken as the upper and lower boundaries, respectively, then the homogeneity range of β-$Zn_{6-\delta}Sb_5$ extends from $Zn_{5.64(1)}Sb_5$ to $Zn_{5.53(1)}Sb_5$ at room temperature. Single-crystal XRD data indicate that the zinc deficiency in single crystals of β-$Zn_{6-\delta}Sb_5$ can be even larger. Because of decomposition of the β-$Zn_{6-\delta}Sb_5$ powder sample at 713 K and limited single-crystal data, we could not verify the $\beta \rightarrow \gamma$ transition temperature of 767 K[15] or check if there are any other polymorphs (Izard et al.[15] reported on two $\gamma \rightarrow \gamma'$ invariant transformations at 798 and 805 K).

High-temperature single-crystal data show that the rhombohedral lattice is still present at 473 and 673 K. The structure (atomic arrangement) similar to that of room-temperature β-$Zn_{6-\delta}Sb_5$ can be assumed at those temperatures. However, nothing can be said about the Zn occupancy. It is likely that zinc sublimation and formation of ZnSb (see below) caused cleavage of the crystal at 673 K, although crystal breaking due to strain effects resulting from thermal expansion of the crystal and/or the capillaries cannot be excluded.

High-temperature powder diffraction data (Table 6) indicate that relatively short heating in dynamic vacuum (data collection at each temperature lasted ~90 min) results in decomposition of the $Zn_{6-\delta}Sb_5$ and $Zn_{1-\delta}Sb$ phases. As evident from the refined compositions of $Zn_{6-\delta}Sb_5$, the β-polymorph starts to lose Zn at 473 K, and after reaching the $Zn_{5.43(2)}Sb_5$ composition, it decomposes into ZnSb and Zn at 623 K. The two reactions can be written as follows:

(a) $Zn_{6-\delta}Sb_5(s) \rightarrow Zn_{6-\delta-x}Sb_5(s) + xZn(g)$

(473−623 K, 10^{-7} Torr dynamic vacuum)

(10^{-7} Torr dynamic vacuum is represented by d.v. later in the paper)

(b) $Zn_{6-\delta-x}Sb_5(s) \rightarrow 5ZnSb(s) + (1-\delta-x)Zn(g)$

(at 623 K, d.v.)

It has to be emphasized that elemental zinc was not detected in the powder sample at high temperatures, which means that it is in a gaseous form. (Sb sublimation from the $Zn_{6-\delta-x}Sb_5$ phase can also occur at high temperature. But since $Zn_{6-\delta-x}Sb_5$ becomes more Zn-deficient with temperature, it is impossible to establish Sb losses from powder XRD. The same argument pertains to the $Zn_{1-\delta}Sb$ phase.) Obviously, there is some homogeneity range in β-$Zn_{6-\delta}Sb_5$ with respect to Zn, but after reaching the minimum Zn concentration, which is 5.43(2) at 623 K for the bulk powder sample, further Zn loss leads to $Zn_{6-\delta}Sb_5$ decomposition (reaction b). On the basis of the diffraction results, it can be concluded that the $Zn_{6-\delta}Sb_5$ phase is kinetically stable under dynamic vacuum with respect to Zn loss (sublimation) up to 373 K. A further temperature increase and possibly longer heating (not tested) produce a zinc-poorer $Zn_{6-\delta-x}Sb_5$ phase and, eventually, the ZnSb phase. This conclusion correlates with the observation made by Tapiero et al., who, using Auger electron spectroscopy, noticed but did not explain strong impoverishment in Zn and a corresponding enrichment in Sb after annealing the Zn_4Sb_3 sample in a vacuum at 673 K (the resulting sample composition was ~27 at. % Zn and ~83 at. % Sb).[11]

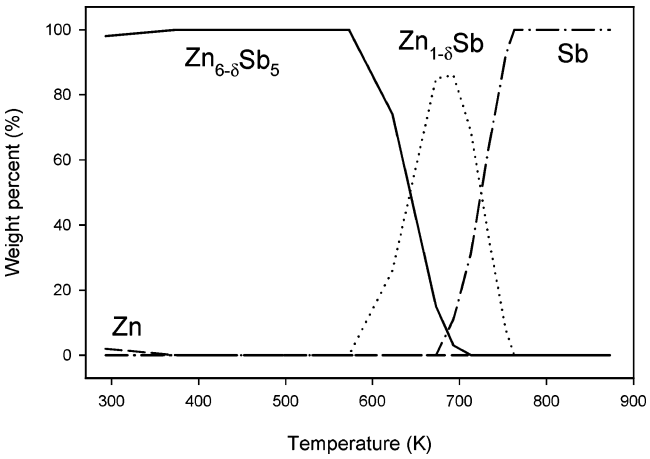

Figure 6. Weight percent of the identified phases in the Zn_4Sb_3 sample during heating (powder XRD data).

The ZnSb phase retains its stoichiometric composition up to 623 K; from 673 K and up, ZnSb loses Zn and becomes nonstoichiometric:

(c) $ZnSb(s) \rightarrow Zn_{1-\delta}Sb(s) + \delta Zn(g)$

(from 673 K up, d.v.)

Similarly to $Zn_{6-\delta}Sb_5$, there seems to exist a maximum Zn deficiency in $Zn_{1-\delta}Sb$ ($\delta = 0.04$) after which the phase decomposes:

(d) $Zn_{1-\delta}Sb(s) \rightarrow Sb(s) + (1-\delta)Zn(g)$

(from 693 K up, d.v.)

The weight percentage of each phase as a function of temperature is plotted in Figure 6 (powder data, accuracy is equal to or less than 1 wt %). The amount of zinc observed at 293 K (1.72(3) wt %) is smaller than the amount expected (6.4 wt %) from the initial composition of the Zn_4Sb_3 sample and the refined composition of the $Zn_{5.64(1)}Sb_5$ phase, assuming no Zn loss during synthesis:

(e) $5Zn_4Sb_3(l) \rightarrow 3\beta$-$Zn_{5.64(1)}Sb_5(s) + 3.08Zn(s)$

Even if Zn losses are assumed because of sublimation, the small volume of the silica jacket used for the synthesis will not account for all Zn lost. It is more likely that "missing" zinc is present as metastable Zn_3Sb_2, whose amount we could not refine due to the lack of its structural data. Elemental zinc found at room temperature was not observed at higher temperatures. However, increase in the Zn occupancy of the $Zn_{6-\delta}Sb_5$ phase at 373 K (Table 6) indicates that some Zn may have entered the $Zn_{6-\delta}Sb_5$ structure, although Zn sublimation may also occur at that temperature. Zinc presence in the Zn_4Sb_3 sample is a known problem: Tapiero et al.[11] reported Zn in the microfissures of the Zn_4Sb_3 alloy prepared in a similar way as ours, and Izard et al.[15] indicated small Zn grains in mechanically alloyed Zn_4Sb_3.

Both groups also found the binary ZnSb phase in the Zn_4Sb_3 samples. Using X-ray diffraction techniques, we did not detect ZnSb in the Zn_4Sb_3 sample, which does

not preclude its presence (the ZnSb amount can be lower than the sensitivity of the methods used). However, we observed a substantial amount of ZnSb (33.8(1) wt %) in the $Zn_{3.6}Sb_3$ sample. These differences in the sample constituents must be due to the compositions of the γ'- and γ-polymorphs, which must be different from that of β-$Zn_{6-\delta}Sb_5$, and due to the $\gamma \rightarrow \beta$ phase transition. Since the Zn_4Sb_3 sample does not have ZnSb but the $Zn_{3.6}Sb_3$ sample does, the compositions of the γ'- and γ-polymorphs must be close to Zn_4Sb_3 to account for the differences in the constituents of the Zn_4Sb_3 and $Zn_{3.6}Sb_3$ samples:

(f) $Zn_4Sb_3(l) \leftrightarrow \gamma'\text{-}Zn_4Sb_3(s)$

(g) $Zn_{3.6}Sb_3(l) \leftrightarrow 0.6\gamma'\text{-}Zn_4Sb_3(s) + 1.2ZnSb(s)$

Reactions (f) and (g) are followed by

(h) $\gamma'\text{-}Zn_4Sb_3(s) \rightarrow \gamma\text{-}Zn_4Sb_3(s)$ (798 and 805 K, simplified)*, then by

(i) $\gamma\text{-}Zn_4Sb_3(s) \rightarrow \beta\text{-}Zn_{6-\delta}Sb_5(s) + Zn_3Sb_2(s)$ (767 K, according to our XRD phase analyses) and

(j) $Zn_3Sb_2(s) \rightarrow \beta\text{-}Zn_{6-\delta}Sb_5(s) + Zn(s)$ (677 K)[15]

(*A detailed description of the $\gamma' \rightarrow \gamma$ phase transition can be found in ref 15.)

While the $Zn_{3.6}Sb_3$ sample will have ZnSb after crossing the liquidus line, the Zn_4Sb_3 sample will not. Once formed, most of the ZnSb will remain since its reaction with elemental Zn, freed in process (j) upon cooling, is likely to be sluggish and incomplete due to a low rate of solid state diffusion, especially during rapid cooling:

(k) $5ZnSb(s) + (1-\delta)Zn(s) \rightarrow \beta\text{-}Zn_{6-\delta}Sb_5(s)$

Reaction (k) was observed by Psarev et al.[5] and Aizawa et al.[26] using XRD powder techniques. The amount of ZnSb formed in reaction (g) would be 37.4 wt %, which is already close to the concentration of ZnSb (33.8(1) wt %) experimentally found in the $Zn_{3.6}Sb_3$ sample. Some reduction of the ZnSb amount can be explained from reaction (k).

Since the compositions of the β-($Zn_{6-\delta}Sb_5$) and γ-polymorphs (Zn_4Sb_3) are different, it is possible that we are dealing with two different phases: low-temperature $Zn_{6-\delta}Sb_5$ stable below 767 K and high-temperature Zn_4Sb_3 existing above 767 K. This is an assumption, which has to be verified using high-temperature XRD techniques. But in light of the data presented here and methods used, it can be difficult to construct and conduct an experiment that will provide adequate crystallographic data.

The $Zn_{6-\delta}Sb_5$ Structure. The relative atomic arrangement in the structure of the room-temperature β-polymorph is similar to that reported by Mayer et al.[10] for "Zn_4Sb_3" but there is no Zn/Sb mixture on any site. Therefore, this structure can be visualized as a 3D network of only Sb atoms with Zn in tetrahedral voids

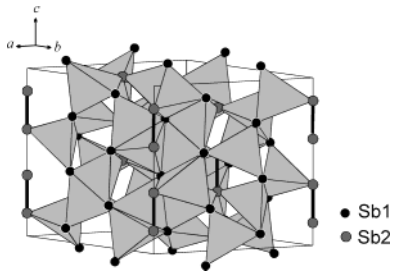

Figure 7. Crystal structure of room-temperature β-Zn_6Sb_5. Zn atoms are inside the antimony tetrahedra. Thick lines indicate the Sb2−Sb2 dimers with bond distances of 2.82 Å.

(Figure 7). The tetrahedra with Sb2−Sb2 edges (d_{Sb-Sb} = 2.82 Å) are not occupied: only tetrahedral units made from Sb1 base and Sb2 apex accommodate Zn atoms. Treating Sb1 atoms as a layer of a close-packed structure that can create twice as many tetrahedral (*T*) voids as there are Sb1 atoms and occupying all these voids with Zn atoms, we can obtain the composition of the nondeficient Zn_6Sb_5 phase: 18 (Sb1 atoms) × 2 (*T* voids/Sb1 atom)/6 (*Z*) = 6 (*T* voids) = 6 (Zn atoms) and [18 (Sb1 atoms) + 12 (Sb2 atoms)]/6 (*Z*) = 5 (Sb atoms). Therefore, the number of zinc atoms is dictated by the presence of two crystallographically and chemically different antimony sites. However, space filling/geometric factors do not indicate whether Zn_6Sb_5 is an electron precise phase. To apply the Zintl−Klemm electron-counting formalism for valence compounds to Zn_6Sb_5,[27] we have to recognize differences in bonding of the Sb1 and Sb2 atoms. The Sb1 atoms have no Sb neighbors and can be treated as Sb^{3-}. The Sb2 atoms form dimers with d_{Sb-Sb} = 2.82 Å, which is characteristic of a Sb−Sb single bond (see, e.g., ref 28), that is isoelectronic with a halogen dimer and carries a formal charge of −2. While three $Sb1^{3-}$ and two $Sb2^{2-}$ in Zn_6Sb_5 require 13 electrons, the fully occupied Zn sites can provide only 6 × 2 = 12 electrons and the deficient Zn site even less. The electron counting and charge assignment become even less clear when the Zn−Zn distances of d_{Zn-Zn} = 2.75 Å between the Zn atoms of the Sb tetrahedra that share edges are considered. These short distances indicate the presence of Zn−Zn interactions that cannot be neglected. Therefore, the Zn_6Sb_5 phase is electron-deficient, and this electron implies partial occupancy of the conductance band and metallic behavior, which agrees with the resistance measurements. The zinc deficiency introduces a local structural disorder, which is likely to decrease both lattice and charge carrier thermal conductivity, and, thus, to contribute to a high *ZT* value as reported for "Zn_4Sb_3". But more detailed analysis of Zn_6Sb_5 electronic structure (band structure calculations) is needed to understand its bonding and role of Zn deficiency.

The $Zn_{1-\delta}Sb$ Structure. The $Zn_{1-\delta}Sb$ structure first reported by Almin[21] (CdSb-type,[29] Figure 8) can be viewed as a hexagonal close packing of Sb atoms in

(26) Aizawa, T.; Iwaisako, Y.; Yamamoto, A.; Ohta, T. *Proc. Int. Conf. Thermoelectrics* **1999**, *18*, 173−176.

(27) Miller, G. J. In *Chemistry, Structure, and Bonding of Zintl Phases and Ions*; Kauzlarich, S. M., Ed.; VCH Publishers: New York, 1996; pp 1−59.

(28) Adolphson, D. G.; Corbett, J. D.; Merryman, D. J. *J. Am. Chem. Soc.* **1976**, *98*, 7234−7239.

(29) Range, K. J.; Pfauntsch, J.; Klement, U. *Acta Crystallogr.* **1988**, *C44*, 2196−2197.

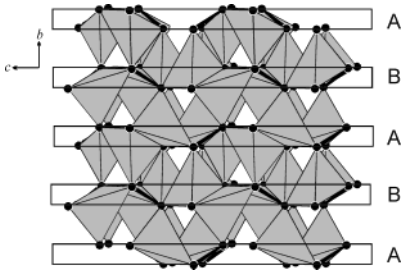

Figure 8. Structure of $Zn_{1-\delta}Sb$ as built from distorted hexagonally close-packed layers of Sb atoms. Zn atoms occupy half of the tetrahedral T_+ and T_- sites. Thick lines indicate the Sb−Sb dimers with bond distances of 2.83 Å.

which the antimony A and B layers are highly puckered. Similarly to β-$Zn_{6-\delta}Sb_5$, $Zn_{1-\delta}Sb$ has both Sb−Sb dimers with $d_{Sb-Sb} = 2.83$ Å (thick black lines in Figure 8) and short Zn−Zn bonds with $d_{Zn-Zn} = 2.84$ Å and appears to be electron-deficient. While in β-$Zn_{6-\delta}Sb_5$ only 2/5 of the Sb atoms make dimers, in $Zn_{1-\delta}Sb$ each Sb atom has a short bond to another Sb atom. As in β-$Zn_{6-\delta}Sb_5$, the tetrahedra, in which a Sb−Sb dimer makes an edge, are not occupied by Zn atoms. The Zn atoms occupy half of the tetrahedral T_+ and T_- sites in a way that each tetrahedron without a Sb−Sb dimer shares all its corners, one edge but no faces with the other units. Since unoccupied tetrahedra with Sb−Sb dimers account for the second half of the T_+ and T_- sites, the number of Zn atoms and, thus, the composition of stoichiometric ZnSb is again "dictated" by the bonding and arrangement of the Sb atoms.

Conclusions

The X-ray diffraction studies undoubtedly indicate that the Zn_4Sb_3 phase does not exist below 767 K, that is, below the "$\beta \rightarrow \gamma$" transition temperature. It is the $Zn_{6-\delta}Sb_5$ phase that is mistakenly assigned the Zn_4Sb_3 composition and is considered to be a promising thermoelectric material. There is no Zn/Sb mixture on any Sb site in the structure of $Zn_{6-\delta}Sb_5$, as previously believed, but there is a significant atomic deficiency on the Zn site. Except for the atomic occupancies, the structure of $Zn_{6-\delta}Sb_5$ is analogous to that reported by Mayer et al. for "Zn_4Sb_3".[10] The $Zn_{6-\delta}Sb_5$ phase has a homogeneity range in Zn, which extends from $Zn_{5.53(1)}Sb_5$ to $Zn_{5.64(1)}Sb_5$ at room temperature for the bulk material. Under dynamic vacuum and at temperatures above 373 K, the $Zn_{6-\delta}Sb_5$ phase loses Zn and eventually decomposes into ZnSb and Zn. This instability can create technological difficulties for obtaining pure samples for industrial applications.

The stoichiometric binary $Zn_{1-\delta}Sb$ phase is also unstable with respect to Zn sublimation at temperatures above 623 K and under dynamic vacuum, which leads to its decomposition into Zn and Sb.

Acknowledgment. This manuscript has been authored by Iowa State University of Science and Technology under Contract No. W-7405-ENG-82 with the U.S. Department of Energy. The research was supported by the Office of the Basic Energy Sciences, Materials Sciences Division, U.S. DOE. Special thanks to Dr. Warren Straszheim for performing EDS analyses and his discussion of the results.

CM035274A